Systemic properties of living cells are the result of molecular dynamics governed by so-called genetic regulatory networks (GRN). These networks capture all possible features of cells and are responsible for the immense levels of adaptation characteristic to living systems. At any point in time only small subsets of these networks are active. Any active subset of the GRN leads to the expression of particular sets of molecules (expression modes). The subsets of active networks change over time, leading to the observed complex dynamics of expression patterns. Understanding of this dynamics becomes increasingly important in systems biology and medicine. While the importance of transcription rates and catalytic interactions has been widely recognized in modeling genetic regulatory systems, the understanding of the role of degradation of biochemical agents (mRNA, protein) in regulatory dynamics remains limited. Recent experimental data suggests that there exists a functional relation between mRNA and protein decay rates and expression modes. In this paper we propose a model for the dynamics of successions of sequences of active subnetworks of the GRN. The model is able to reproduce key characteristics of molecular dynamics, including homeostasis, multi-stability, periodic dynamics, alternating activity, differentiability, and self-organized critical dynamics. Moreover the model allows to naturally understand the mechanism behind the relation between decay rates and expression modes. The model explains recent experimental observations that decay-rates (or turnovers) vary between differentiated tissue-classes at a general systemic level and highlights the role of intracellular decay rate control mechanisms in cell differentiation.

Introduction

Understanding living cells at a systemic level is an increasingly important challenge in biology and medicine [1–5]. Regulatory interactions between intracellular molecular agents (e.g. DNA, RNA, proteins, hormones, trace elements), form so-called *genetic regulatory networks* (GRN), which orchestrate gene expression and replication, coordinate metabolic activity, and cellular development, respond to changes in the environment, or stress. GRN coordinate regulatory dynamics on all levels from cell-fate [6, 7] to stress response [8–10]. Qualitative understanding of GRN topology is for instance obtained from promoter sequences [11–13], gene-expression profiling [14–16] or protein-protein interactions (proteome) [17]. However qualitative information on GRN topology alone is insufficient to understand GRN dynamics. It has been recognized that quantitative information is required to understand the complex dynamical properties of regulatory interactions in living cells [18,19], mainly because dynamics on interaction networks with identical topology still depends on the strength of interactions (links) between agents (nodes). Models of GRN dynamics aid the task of understanding properties of GRN at various levels of detail available in experimental data and therefore provide valuable tools for integrating information from different sources into unifying pictures and for reverse engineering GRN from experimental data. Any model should *adequately* reproduce GRN dynamics and *sufficiently* exhibit systemic properties of the GRN, including homeostasis, multi-stability, periodic dynamics, alternating activity, self-organized critical dynamics (SOC) and differentiability.

Homeostatic dynamics regulates the equilibrium concentration levels of agents, e.g. [20], *multi-stability* shows switching between multiple steady states [21,22]. Examples for *periodic dynamics* are e.g. the cell-cycle [17], circadian-clock [23], IκB-NκB signaling [24], hER dynamics [25,26] etc. Some molecular agents show *alternating activity*, i.e. their concentrations alternate between being detectable (on) and below detection threshold (off), see e.g. [25,26]. *Self-organized critical* (SOC) dynamics corresponds to details of regulatory dynamics ensuring (approximate) stability within a fluctuating environment through various mechanisms of adaptation. Finally the property of *differentiability* means that cells of multicellular organisms can differentiate into various cell-types (liver, muscle, blood, kidney, cancer, ...). The differentiated cells possess identical GRN but express distinguishable patterns of regulatory activity. The same GRN therefore can be expressed in different *modes* so that some agents become expressed in one mode but not in another [27].

Recently it has been reported that both regulation of transcription and mRNA decay rates (i.e. the mRNA turnover) are necessary to understand experimentally observed expression values [28]. Moreover it has been demonstrated that decay rates of mRNA are cell-type specific [29]. Analogously for proteins, where the dominant mechanism is the Ubiquitin driven proteolyse in the Proteasom [30], protein abundance and therefore their degradation has to be tightly controlled [31]. Also the abundance of proteins and whether certain proteins are produced or not is again cell-type specific [32,33]. This indicates that decay-rates and their control play a crucial role in cell-differentiation.

Variable decay rates however and the property of differentiability are hardly ever considered in GRN models where decay rates of agents are usually kept constant. Understanding the effects of changes of decay rates of agents therefore is a crucial step towards a deeper understanding of GRN dynamics and the role decay rates play in cell-differentiation. The GRN is the set of all possible interactions of molecular reactions and bindings. The GRN captures all possible features of cells and are responsible for the immense levels of adaptation characteristic to living systems. What happens when different cell-types express the same GRN in alternative ways? At any point in time only small subsets of the GRN are active. Any active subset of the GRN leads to the expression of particular sets of molecules (expression modes). The *active regulatory network* at time t is the regulatory sub-network of the GRN, governing the molecular (auto-catalytic) dynamics of all agents which exist at time t. The set of existing molecules forms the *active agent set* at time t. The active network changes over time and typical sequences of active sets represent what we call the *expression modes* of a specific cell-type and their cell-cycle. Expression modes themselves can be modified, either locally as a reaction to an external signal, or fundamentally through further cell differentiation. Active sets of molecules are transient and what is observed in experiments is a superposition of subsequent active sets, which we call the *expressed set of agents* and the regulatory interactions between the expressed agents the *expressed regulatory network*. To find the property of differentiability in a regulatory network model therefore requires that one network is capable of producing different expression modes while perturbations (external signal) only modify active sets locally and the particular expression mode can be restored.

The six dynamical properties we have listed above have been addressed with a variety of conceptually different models. The essence of all these models is that they try to capture the dynamics induced by positive and negative feed back loops within the GRN. The choice of model depends largely on the type and resolution (coarse graining) of experimental data. At the single cell level cellular activity (e.g. concentrations x_i of biochemical agents i) can be modeled by non-linear (stochastic) differential equations [34, 35] which can explain homeostasis, periodic and multi-stable behavior. The dynamics governed by a GRN is given by a set of coupled non-linear differential equations

$$\dot{x}_i = F_i(x)\,, \tag{1}$$

where F_i is a (non-linear) function capturing the GRN. It depends on the vector of concentrations of all the possible N molecular agents in a cell, $x = \{x_i\}_{i=1}^{N}$. $\dot{x}_i$ is the time derivative of the concentrations x_i. Note that F_i can have stochastic components. Analysis of such systems is often complicated by the interplay between fluctuations and non-linearities [36].

Differential equation models can be approximated by cellular automata, Boolean or piecewise-linear models. The property of SOC dynamics, or dynamics at the "edge of chaos" [37–39], has been studied mainly in the context of cellular automata and Boolean models [40–42]. SOC dynamics was also discussed in continuous differential equation based models [43, 44]. Boolean and piecewise-linear models share common origins in the work of Glass and Kauffman, [45], and have extensively been used for modeling and analyzing GRN [46–49]. For their superior properties in approximating non-linear systems (in principle to any suitable precision) piecewise-linear models also are applied in different disciplines, for instance for modeling highly non-linear electronic circuits [50].

In the context of GRN both boolean and piecewise-linear models usually are used for describing non-linear dynamics with switch-like regulatory elements frequently observed in biological regulatory processes [51, 52]. Such switches react if the concentration of an agent (the signal) crosses a specific threshold level. To model such switches in regulation networks of N molecular agents with concentrations x_i the space of concentrations $\mathcal{D} = \{x | x_i \geq 0\}$ is cut into segments defined by the threshold values where the concentration x_i can trigger a regulatory switch. These segments are called *regulatory domains* (e.g. [53]). In each such domain Eq. (1) gets approximated by a linear equation of the form

$$\dot{x}_i = \Phi_i + \sum_{j=1}^{N} A_{ij} x_j \ , \tag{2}$$

where the $\Phi_i > 0$ are production rates and A_{ij} are interaction matrices between agents. If $A_{ij} > 0$, then j promotes the production of i. If $A_{ij} < 0$, then j suppresses i. If $A_{ij} = 0$ j has no influence on i. The diagonal elements $A_{ii} < 0$ are *decay rates*, $D_i = -A_{ii}$. Non-linear effects purely come from concentration x_i passing threshold levels, where the dynamics of x_i switches from one to another regulatory domain with different values of Φ and A_{ij}. Equation (2) is a slight generalization of the Glass-Kauffman PLM, [45,53], where $A_{ij} = 0$ except for the (usually) fixed decay rates D_i, so that only the production rates change with the regulatory domain.

Given that the interaction matrix A of the regulatory network is invertible (which is almost certainly true for the biologically relevant range of connectivities of GRN) Eq. (2) can be rewritten

$$\dot{x}_i = \sum_{j=1}^{N} A_{ij} \left(x_j - x_j^* \right) \ , \tag{3}$$

with x^* being the solution of the equation $\Phi_i = -\sum_j A_{ij} x_j^*$. The fixed-point x^* is stable (unstable) and x_i will be attracted (repelled) by x_i^*. If x^* is stable and $x_i^* > 0$ for all i then $x(t) = x^*$ is a stationary solution of Eq. (2).

Not all models approximating nonlinear differential equation descriptions of GRN are equally suited to capture all GRN properties discussed above simultaneously depending on whether discrete (Boolean, cellular automata) or smooth (differential equation) features dominate the model. However there exists a surprisingly simple class of models which exhibits *all* desired GRN properties.

Here we present such a simple model that captures all of the above dynamical properties. We find that the alternating dynamics plays a key role for the stability of regulatory systems and for the formation of SOC dynamics in particular [43, 44]. Most importantly we are able to show that even unspecific control over decay rates, changing the magnitude of all decay rates simultaneously by a (small) factor, leads to "cell differentiation", i.e. the same regulatory network enters different expression modes, displaying different sequences of active regulatory networks.

We show that experimental facts, linking variations of decay rates observed between different cell-types of an organism to variations of the abundance of intra-cellular biochemical agents in these cell-types, correspond to (a) differences in the *expressed* genetic regulatory network, and (b) these differences can be controlled via decay rates of intracellular agents. In other words typical expression modes (cyclical

sequences of successive active sub-networks of the GRN) can be altered and switched by controlling decay rates.

The model

Glass-Kauffman systems, [45], produce positive concentrations $x_i(t) > 0$ for all times t given positive initial conditions $x_i(0) > 0$. This however makes it impossible to produce alternating activity of agents since zero-concentrations $x_i(t) = 0$ can not appear. Therefore we have to generalize Glass-Kauffman systems to more general forms of invertible interaction matrices A_{ij} where the positivity of solutions of Eq. (2) is not implicitly guaranteed, but where positivity (non-negativity) is ensured as a constraint to the system,

$$x_i(t) \geq 0 \quad \forall \text{ agents } i, \text{and times } t \quad . \tag{4}$$

This constraint alters the linear dynamics of Eq. (2) in the following way. Whenever a concentration x_i becomes zero at time t then $x_i(t')$ remains zero for $t' > t$ for as long as $\dot{x}_i(t') < 0$, according to Eq. (2). If $\dot{x}_i(t''') \geq 0$ for $t''' \geq t'' > t$ then $x_i(t''')$ is no longer subject to the positivity constraint and continues to evolve according to Eq. (2) again. Agent i is said to be *active* at time t, if $x_i(t) > 0$ and *inactive*, if $x_i(t) = 0$.

The positivity constraint Eq. (4) implies the following consequences. At any point in time there will be a sub-set of agents with non-vanishing concentrations which we call the *active set* of agents. The remaining agents have zero concentration, and therefore do not actively influence the concentrations of any of the non-vanishing agents. There exist 2^N different active sets, i.e. 2^N combinations in which N agents can be active or inactive. Each active set can be uniquely identified by an index $s = 1, \ldots, 2^N$. In the course of time t some agents will vanish while others re-appear, so that one effectively observes a sequence of sets of active agents

$$s_0 \overset{t_1^{\text{switch}}}{\longrightarrow} s_1 \overset{t_2^{\text{switch}}}{\longrightarrow} s_2 \overset{t_3^{\text{switch}}}{\longrightarrow} \ldots , \tag{5}$$

s_0 being the initial active set. The active set s_{m-1} switches to active set s_m at time t_m^{switch}. In each time interval $T_m = \left[t_m^{\text{switch}}\, t_{m+1}^{\text{switch}}\right]$ of duration $\tau_m = t_{m+1}^{\text{switch}} - t_m^{\text{switch}}$ it is thus possible to only consider the regulatory sub-network acting on the set of active agents s_m. This sub-network is described by the part of the full interaction matrix A_{ij}, where i and j are restricted to the set of active agents s_m. These sub-matrices we call *active networks* and denote them by $A_{\text{act}}^{s_m}$. The concentration vector of active agents we call $x_{\text{act}}^{s_m}$. Active agents also "feel" a modified *effective* fixed point $x_{\text{act}}^{*\,s_m}$, such that finally for $t \in T_m$ the concentrations of the active agents follow a linear equation

$$\dot{x}_{\text{act},\,i}^{s_m}(t) = \sum_{j \text{ is active}} A_{\text{act},\,ij}^{s_m} \left(x_{\text{act},\,j}^{s_m}(t) - x_{\text{act},\,j}^{*\,s_m}\right) . \tag{6}$$

We refer to such systems as *sequentially linear* systems. The attractiveness of this description arises through the fact that it becomes possible to understand the dynamics by considering the sequences of active networks

$$A_{\text{act}}^{s_0} \overset{t_1^{\text{switch}}}{\longrightarrow} A_{\text{act}}^{s_1} \overset{t_2^{\text{switch}}}{\longrightarrow} A_{\text{act}}^{s_2} \overset{t_3^{\text{switch}}}{\longrightarrow} \ldots , \tag{7}$$

which allows to analyze dynamical properties in terms of eigenvalues and eigenvectors of the active sub-matrices $A_{\text{act}}^{s_m}$ (see Materials and Methods). This model can be shown to be mathematically equivalent to [43, 44].

Cell differentiation in the sequentially linear dynamics

In the picture of sequentially linear dynamics it becomes possible to identify operational modes of a cell as a particular sequence of active networks. Cell types in ordinary operational modes may be classified by

specific sequences. As a hypothetical example a liver cell under typical conditions might be characterized by a *periodic* sequence $A^9_{\rm act} \to A^{10}_{\rm act} \to A^{46}_{\rm act} \to A^2_{\rm act} \to A^9_{\rm act}$, whereas an endothelial cell is given by $A^{123}_{\rm act} \to A^2_{\rm act} \to A^4_{\rm act} \to A^{209}_{\rm act} \to A^9_{\rm act} \to A^{77}_{\rm act} \to A^{123}_{\rm act}$. Note that all types share the same full regulatory network A. This separates timescales of the dynamics: on the fast timescale the dynamics is continuous and characterized by linear changes of the concentrations x_i. On the slower time-scale the dynamics is characterized by discrete changes of active sets. The change from one sequence of active sets to another can be interpreted as the expression modes of different cell-types (cell differentiation) and we show that changes in decay rates of molecular species trigger switches between expression modes.

Example

As an example for sequentially linear dynamics we consider a system with $N = 4$ molecular agents, $x^*_i = 100$, $D_i = -A_{ii} = 0.23$ for all agents $i = 1, \ldots, 4$, and a regulatory network given by

$$A = \begin{pmatrix} -0.23 & -0.1 & 0 & 0.1 \\ 0 & -0.23 & 0.2 & 0 \\ 1 & 0 & -0.23 & -1 \\ -0.8 & -0.8 & 0.1 & -0.23 \end{pmatrix}. \tag{8}$$

The dynamics of this system (over one period) is shown in Fig. 1 a. The property describing the stability of an active set s_m is the maximal real part of the eigenvalues $\Lambda^{s_m}_{\rm act}$ of the active matrix $A^{s_m}_{\rm act}$ denoted $L^{s_m}_{\rm act} = \max \mathrm{Re}(\Lambda^{s_m}_{\rm act})$. The number q denotes the number of time-domains in a periodic sequence of active networks and z is the number of different sub-networks that are activated in a sequence (see also materials and methods). In this example there are four time-domains ($q = 4$) associated with three different active sets ($z = 3$) which are periodically repeated. The sequence starts in time-domain 1 with active set $s = 1$ with maximum real eigenvalue $L^1_{\rm act} = 0.03$. Positive $L^1_{\rm act}$ means that the fixed point of the active set is unstable and the associated leading eigenvalue implies that the concentration of one agent (green) is decaying to zero. The positivity condition deactivates this agent as its concentration becomes zero and the system enters time-domain 2 as the active set switches to $s = 3$ with $L^2_{\rm act} = -0.24$. Negative $L^2_{\rm act}$ means that the fixed point $x^{*\,3}_{\rm act}$ is stable and $x^2_{\rm act}$ tries to approach $x^{*\,2}_{\rm act}$. This leads to the deactivated agent (green) becoming produced again and the system switches back to $s = 1$ entering the third time-domain. In time-domain 3 the initial conditions differs from the one in time-domain 1 and a different node (magenta) gets deactivated. The system switches to $s = 2$ with $L^3_{\rm act} = -0.09$ at the beginning of the fourth time-domain. This means $x^{*\,2}_{\rm act}$ is a stable fixed-point and the inactive node (magenta) eventually gets produced again as the system switches back to the beginning ($s = 1$) and enters the next period. The system is thus precisely characterized by the sequence $A^1_{\rm act} \to A^3_{\rm act} \to A^1_{\rm act} \to A^2_{\rm act} \to A^1_{\rm act}$. The eigenvalue spectra of the sub-matrices $A^{s_m}_{\rm act}$ associated with subsequent time-domains T_m are shown in Fig. 1 b. Fig. 1 c shows a projection of the trajectory into a three dimensional Poincare map. Fig. 1 d shows the eigenvalue spectra of the different active sub-systems of the dynamics.

Some details of the dynamics, like the existence of multiple stable fixed-points, the periodicity of bounded attractors and temporal self-organization, can be mathematically fully understood. In [43, 44] it was already shown mathematically that sequentially linear models exhibit *homeostasis*, *multi-stability*. This has been demonstrated for a wide range of system size N, and a number of interactions (connectivity) and fixed decay rates. *Periodic dynamics*, and *self-organized critical* dynamics have been noted in [43,44] but were not clarified and require further explanation which is given in detail in the materials and methods, where also a simple temporal balance condition is described and derived.

The temporal balance condition states that the time-average over the real parts of the leading eigenvalues $L^{s_m}_{\rm act}$ of the matrices $A^{s_m}_{\rm act}$ in a sequence of active networks approximate the Lyapunov exponent λ. The Lyapunov exponent λ measures the overall stability of a system ($\lambda < 0$ stable, $\lambda > 0$ instable, $\lambda = 0$ critical) and for sequences following a periodic attractor λ can be shown to be exactly zero. Inserting the values for τ_s and $L^s_{\rm act}$ from table (1) into the balance condition, Eq. (10) gives the value -0.055 as

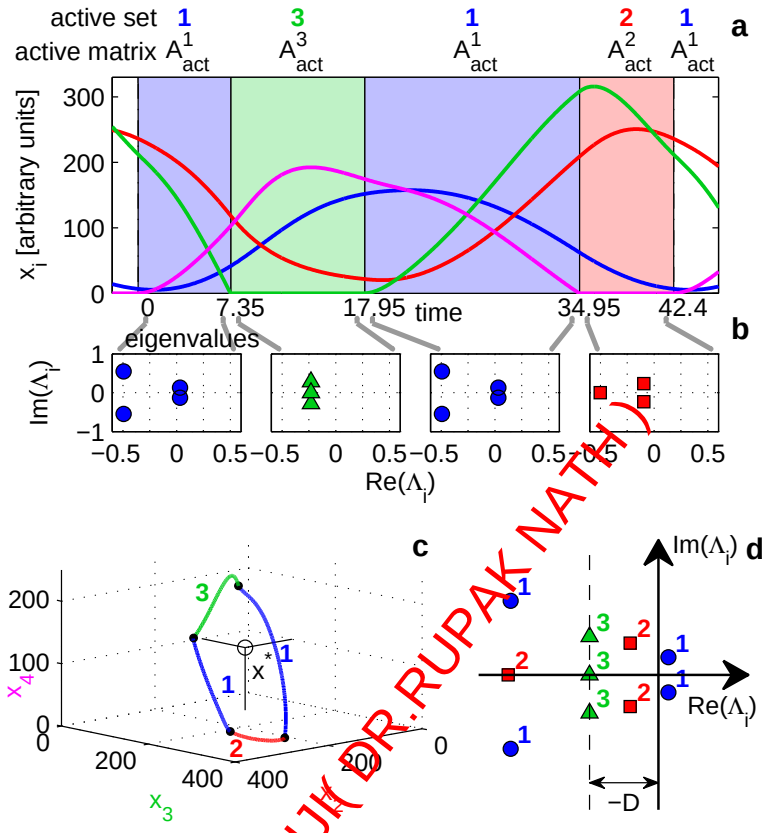

Figure 1. Periodic dynamics and active sets. Sequentially linear system with decay rate $D_i = 0.23$ and the fixed point $x_i^* = 100$ for all agents i simulated with time-increment $dt = 0.05$. Periodic time-series organized into a sequence of four domains with three different active sets. For each time-domain the associated spectrum of eigenvalues for the active sets is shown in (b). In (c) a 3d Poincare map of the limit cycle is plotted together with the projection of x^* in the center. The domains are marked with bold numbers and switching events with dots. (d) The eigenvalue spectra of the different subsystems are plotted in the imaginary plane. The shift of the spectrum along the real axis depending on the decay rate D is indicated.

an approximation of λ (which has an exact value of zero). Although the balance equation gives only a crude approximation of the Lyapunov exponent it allows to understand why the example-system spends more time in the weakly instable time-domain 1 and 3, than in the stable time-domains 2 and 4 which is obviously true from Fig. 1. Strong convergence needs less time to compensate for weak divergence.

Temporal balance is a consequence of the mechanism of self-organization that fine-tunes switching times such that stable parts of the dynamics compensate instable parts of the dynamics exactly. This mechanism can be understood in the following way. Sequentially linear systems try to converge to a fixed point. If it is reached the system becomes static. The fixed point might not be *accessible* however, meaning that the trajectory on the way toward the fixed point hits a boundary (Fig. 1 c) causing a switching event which changes the dynamics so that the system now is attracted by a different effective fixed point, which it tries to reach. If the system does not converge to an accessible fixed point it is either unstable and some concentrations x_i diverge, or the system circles through some of the 2^N possible active

time-domain	s	$N_{\rm on}$	τ_s	$L^s_{\rm act}$	stability
1	1	4	7.35	0.033	unstable
2	3	3	10.6	-0.24	stable
3	1	4	17.0	0.033	unstable
4	2	3	7.45	-0.094	stable

Table 1. Properties of 4-node example system. Some characteristics of the four node system shown in Fig 1 are listed, including the index of the time domain, the index of the sub-system s, the number of active nodes $N_{\rm on}$, the time the system spends in the s'th sub-system, the real-part of the leading eigenvalue of s, and whether sub-system s is stable or not.

sets and converges onto an effective attractor - characterized in the sequence of active networks. In the later case small perturbations of $x(t)$ on the attractor will vanish with time. This allows to show that bounded dynamics that does not converge to a fixed-point has to be periodic (materials and methods). Switching times are not static but react to perturbations of concentrations x_i. Perturbations shift the occurrence of switching times proportional to the magnitude of the perturbation. This has the effect that switching events act like sliding "focal planes" allowing the perturbed dynamics to "refocus" onto the periodic attractor. While the perturbed dynamics returns to the attractor switching times cumulate small time-shifts resulting in a phase-shift of the periodic dynamics. A perturbation is remembered as a phase-shift of the periodic dynamics which neither grows exponentially nor dies out. The Lyapunov exponent therefore is zero and the systems self-organizes to the "edge of chaos" by adaptation of switching times. Stable adaptive dynamics is a result of this "temporal self-organization".

Results

We first show that the model is able to explain actual empirical data, including alternating dynamics. Figure 2 shows data of molecular concentrations $x_i(t)$ (hERα (black), Pol II (red), TRIP1 (blue), HDAC1 (green)) over three periods of about 40 minutes time. These four agents are all part of the human estrogen nuclear receptor dynamics. The source of the Data is Metivier et. al. [25]. Data points were taken from Pigolotti et al. [54] and the actual values of the matrix elements

$$A = \begin{pmatrix} -1.08 & 1.6 & 0 & 0 \\ 0 & -1.08 & 1.7 & 0 \\ -2.2 & 0 & -1.08 & 2.7 \\ -1 & 0 & 0.1 & -1.08 \end{pmatrix} \tag{9}$$

are bests fits with identical decay rates for optimal explanation of the data. The TRIP1 data (blue) shows *alternating activity* which is reproduced perfectly by our sequential linear model.

Decay rates and expression modes

In the following we show how the change of decay rates induces changes from one cell-type to another. In particular we show how changes of the overall strength of the decay rates results in differentiated dynamics, i.e. in distinct sequences of active expressed networks. This allows to understand recent experimental observations which indicate correlations between cell-type, expressed sets of agents, and decay-rates [27–29, 31–33].

For a fixed interaction network temporal self-organization can be maintained for a wide range of decay rates D. We show this in the same 4-node system considered in Fig. 1 by only varying the decay rate

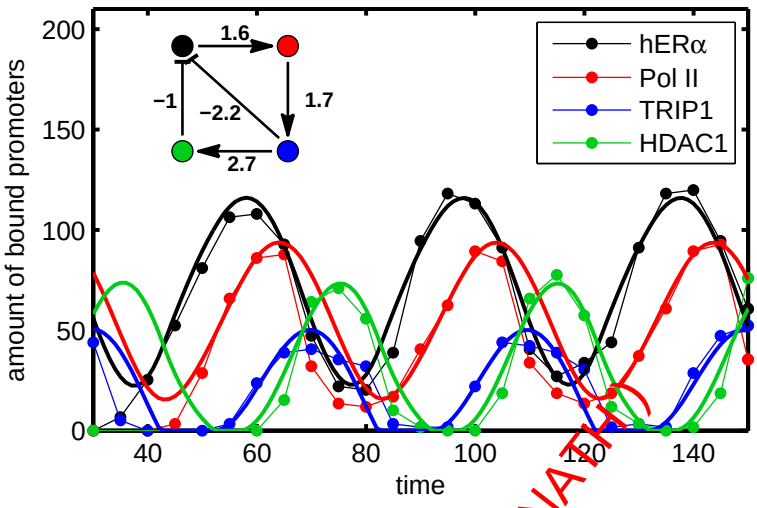

Figure 2. Adequacy of sequentially linear systems. Time series of periodic binding of four proteins to the pS2 promoter after addition of estradiol - experimental data has been extracted from [54], where a negative feedback-loop was proposed to explain the dynamics. Experimental data due to [25] and [26] (dotted lines) is compared with a simulation of a SL system, based on the network shown in the inset, with uniform decay rates $D_i = 1.08$ for all agents and fixed point concentrations $x^* = [75; 60; 20; 30]$. Correlation coefficients for simulated and measured time-series are $C_i = (0.97; 0.84; 0.94; 0.97)$ for time larger 40 and agents i in order of the legend. The model simulation uses zero concentrations for all agents as initial condition and a time increment $dt = 0.1$. For matching the simulation with experiment time in the model is shifted by -40.

$D = -A_{ii}$ from Eq. (8). Figure 3 a shows the Lyapunov exponent λ as a function of D. A plateau, where $\lambda \sim 0$, is clearly visible. If the decay rate is larger than a critical value $D > 0.26$, the Lyapunov exponent becomes negative ($\lambda < 0$) and the system stable. If the decay rate is smaller than a critical value of $D < 0.06$, temporal balance can not be achieved any more, refocusing breaks down, and the system becomes chaotic and trajectories diverge exponentially with $\lambda > 0$. In Fig. 3 b the length of the periodic sequences q (green triangles), which is the number of time-domains in a sequence, and the number z of different active sets activated in this sequence (red squares) is depicted. Figure 3 b also shows that at several critical values of $D \sim 0.088, 0.162, 0.171, 0.224, 0.246, 0.263$ in the plateau region the sequences of active regulatory sub-networks changes when temporal balance can no longer be established merely by adapting the switching times of a sequence. Sequences do not usually change completely at critical values of D and are only expanded by additional active subsets. This can be seen clearly in the 3D Poincare map of the dynamics Fig. 3 d, where the sequence of subsystems s given by $1 \to 2 \to 1 \to 3 \to 1$ (for $D = 0.23$) gets expanded to the sequence $\mathbf{1} \to \mathbf{2} \to 10 \to 9 \to \mathbf{1} \to \mathbf{3} \to 7 \to 5 \to \mathbf{1}$ (for $D = 0.14$). In the materials and methods, Fig. (1), the longer sequence is also shown in the space of all possible active sets. The mathematical reason why such critical decay rates exist is that changes of D shift the eigenvalue spectra of the active interaction matrix $A^s_{\rm act}$, shown in Fig. 3 e, along the real axis. The real part of the leading eigenvalues, $L^s_{\rm act}$, is becoming smaller (larger) than zero and $x^{*\,s}_{\rm act}$ becomes an attractor (repellor) of $x^s_{\rm act}$. The stable fixed point then either is accessible and the dynamic changes from periodic to stationary or inaccessible and the dynamic changes qualitatively but remains periodic. Which agents become active in a given active set s is depicted in Fig. 3 b for three different sequences of active sets

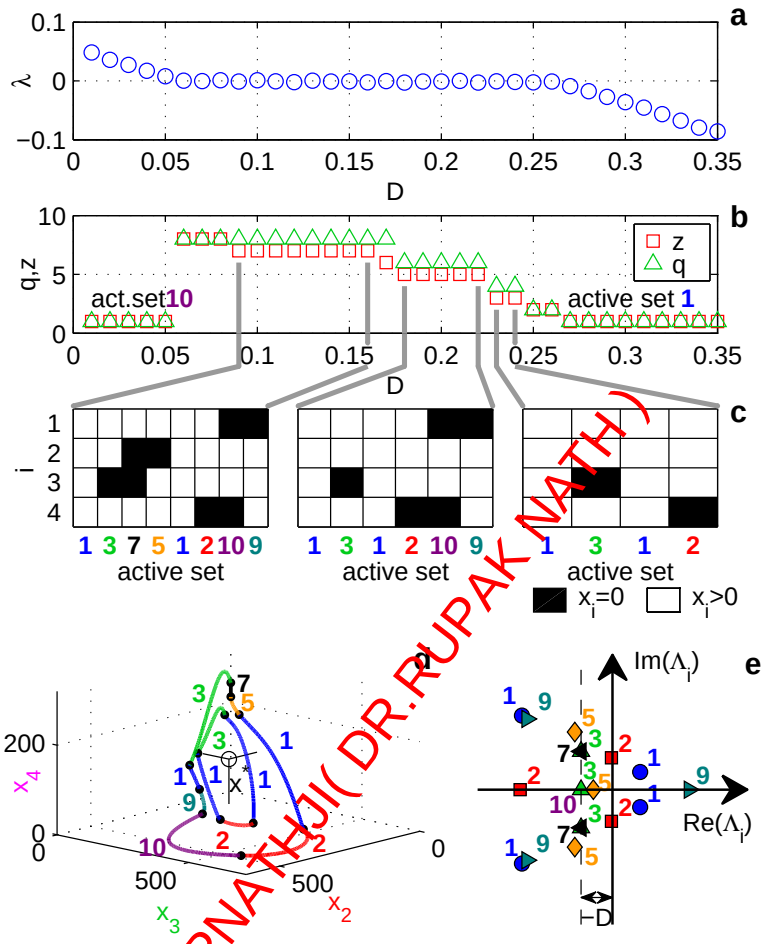

Figure 3. The edge of chaos. The Lyapunov exponent λ of the four node system, Eq. (8), is shown in (a) as a function of the decay rate D, which exhibits a "plateau" with $\lambda = 0$ in the range $0.06 < D < 0.26$. In (b) the length q of the periodic sequence of domains is plotted in green triangles and the number of different active sets z as red squares. In (c) the sequences of active sets are shown for decay rates $D = 0.23$, $= 0.2$ and 0.14. The limit circles for decay rates $D = 0.23$ (short sequence) and $D = 0.14$ (long sequence) are visualized in (d) in a Poincare map using three out of four phase-space dimensions. With decreasing D the radius of the limit circle becomes wider and additional sets (marked with colors) become active. In (e) the spectra of eigenvalues are shown for all the appearing active sets with $D = 0.14$.

associated with three different ranges of the decay rate D indicated by gray lines. If node i is active in active set s then the associated field is white and black otherwise.

The number of *expressed* agents $N_{\rm exp}$ is the number of agents that are active at least once during a period of the dynamics. To demonstrate that not only the periodic activation of agents depends on D but also the number of expressed nodes $N_{\rm exp}$ itself, we consider a larger sequentially linear system with $N = 50$ agents. The interaction matrix of the system is a random matrix with average connectivity $\langle k \rangle = 10$, meaning for each node 10 interactions with other agents have been randomly chosen with equal

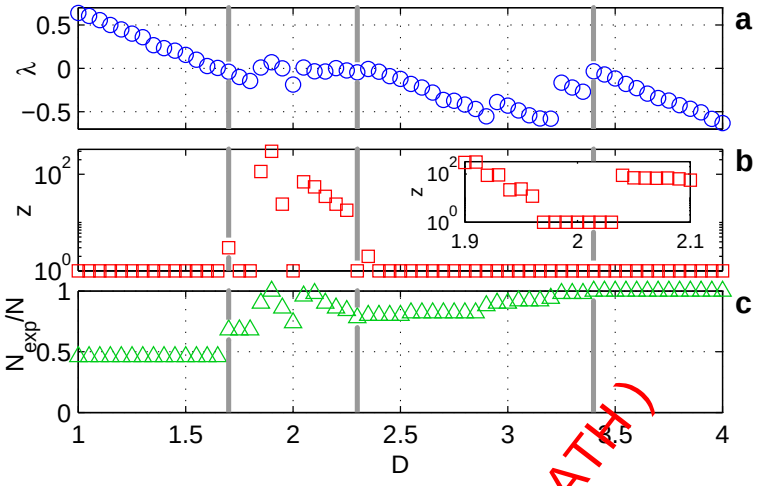

Figure 4. Degradation rates and active networks. Example of a SL system with $N = 50$ and $\langle k \rangle = 10$ and identical initial conditions for all values of D. (a) The Lyapunov exponent, (b) the number of active sets z in a period (if $z = 1$ then the the sequence is not periodic but a steady state!), and (c) the fraction of expressed nodes are plotted as functions of the uniform decay rates $D_i = D$. For $D > 3.4$ x^* is stable. In the range $2.4 < D < 3.4$ the x^* has become unstable but the plateau ($\lambda = 0$) can not form since the dynamic finds active sets s with stable and accessible $x^{*\,s}_{\rm act}$. The inset in (b) shows that in the plateau region a small window, $1.97 < D < 2.03$, exists where again an active set s contains an accessible $x^{*\,s}_{\rm act}$ attracting the dynamics. In the range $1.7 < D < 2.4$ the plateau forms and dynamics gets periodic. For $D < 1.7$ the system gets unstable.

probability. Each non-zero entry, describing such an interaction, is drawn from a normal distribution with mean zero and a standard deviation of $\sigma = 1$. This means that the interaction strength is of magnitude 1 on average and has positive or negative sign with equal probability. In Fig. 4 a the Lyapunov exponent λ, in Fig. 4 b the number z of sets that become active during a cycle and in Fig. 4 c the fraction of expressed agents $N_{\rm exp}/N$ is plotted as a function of D. For large decay rates ($D > 3.4$) the system is stable and x^* is a fixed-point of the dynamics. As D decreases x^* becomes unstable for $D \sim 3.4$. However for $2.3 < D < 3.4$ the system ends up in some stable accessible fixed point $x^{*\,s}_{\rm act}$ so that $x(t)$ approaches a stationary state and $z = 1$. In this range $N_{\rm exp}$ increases with D. The $\lambda \sim 0$ plateau with stable self-organized critical dynamics ($z > 1$) only emerges in the range $1.7 < D < 2.4$ where number of active sets z and expressed network size $N_{\rm exp}/N$ vary strongly. $N_{\rm exp}/N$ varies between 1 and 0.5 which means that changes of the decay rate can induce changes of the size of the expressed network comparable to the magnitude of the full interaction network. A small window of stability exists for $1.97 < D < 2.03$ (see inset).

The strong dependence of $N_{\rm exp}/N$ on the decay-rate D (up to 50% of the total regulatory network) demonstrates clearly that decay-rates alone massively influence sequences of active systems without changing the interaction strength between agents in the regulatory network at all. Moreover, decay rates can also cause switches between fixed-point dynamics and periodic dynamics. While fixed points favor larger decay-rates (in the example $D > 2.3$) there can also exist fixed points for smaller decay rates (window of stability $1.97 < D < 2.03$) where systems favor periodic dynamics.

Discussion

We presented a model which de-composes the dynamics of molecular concentrations – governed by the full molecular regulatory networks – into a temporal sequence of active sub-networks. This novel type of model allows not only to reduce the vast complexity of the full regulatory network into sub-networks of managable size but further to approximate the complicated dynamics by linear methods. The intrinsic non-linearities in the system which lead to alternating dynamics in concentrations (as found in countless experiments) are absorbed into switching events, where the dynamics of one linear system switches to another one. In this view different cell types correspond to different sequences of active sub-networks over time.

These sequentially linear models allow not only for the first time to describe all the relevant dynamical features of the GNR (homeostasis, multi-stability, periodic dynamics, alternating activity, differentiability, and self-organized criticality), but also offers the handle to understand the role of molecular decay rates. The fact that sequentially linear dynamics properly models homeostasis, multi-stability and periodic behavior was shown in [43, 44]. Here we have shown how self-organized criticality (Lyapunov exponent self-regulates to zero) arises as a consequence of temporal balance of switching events. This requires agents to show alternating activity (being repeatedly on and off), which is a natural property by construction of sequentially linear models, and which has posed an unresolved problem of previous models such as the Glass-Kauffman [45] model and its many variants. The mechanism behind self-organized criticality is based on adaptive switching times which effectively lead to refocusing of perturbed dynamics onto the attractor of sequences of active sub-networks. Such a temporal self-organization causes long time memory of perturbations in terms of phase-shifts of the otherwise unchanged periodic dynamics, causing the Lyapunov exponent to become zero. In other words slight perturbations, e.g. noise, only cause time-shifts of the sequence of regulatory reactions but do not change the underlying sequence. Perturbations are "remembered" by the system by non vanishing phase-shifts and the dynamics gets "refocused" onto the periodic attractor merely accumulating a time-shift. This has the consequence that the Lyapunov exponent is zero and the system self-organizes its criticality by adapting switching-times. Practically this means that a system balances the time it spends in its active sub networks with stable and unstable dynamics (temporal balance).

Applying the sequentially linear model to the problem of cell-differentiation we demonstrate that different levels of decay rates are one to one related with transitions from one active sub-network sequence (cell type) to another. This might be a key ingredient to understand a series of recent experimental facts reported on the role of decay-rate regulation systems and the role of noise in cell differentiation [27–29, 31–33]. We found that by varying the decay rates only, while keeping the complete regulatory network fixed over time, substantially modifies the temporal organization of regulatory events. In particular the decay rate controls the number of expressed agents, the sequence of active sub-networks, and sometimes even the type of solution (stable, stationary, periodic). The changes occur at critical levels of decay rates and changes can be drastic. For example we find situations where a 5% variation of the decay rate causes an approximate doubling of the number of expressed agents. This demonstrates that different expression modes, which distinguish different cell-types from each other, can be very efficiently obtained by controlling the decay rates of agents without altering any interactions between agents in the regulatory network, which is very costly in an evolutionary sense. These findings highlight the importance of intracellular decay rate control mechanisms and the role of noise in cell differentiation.

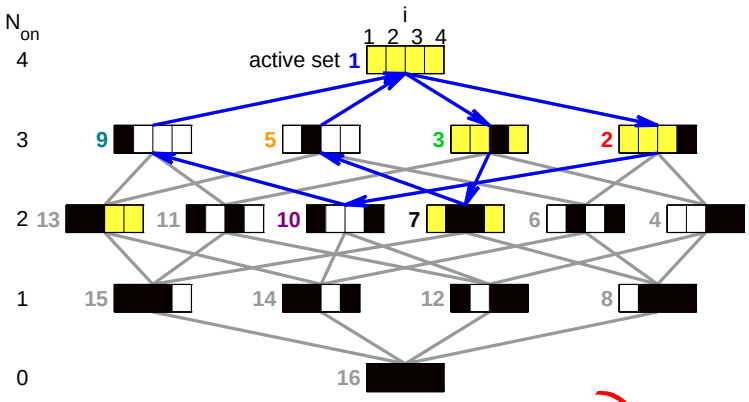

Figure 5. Tree of active sets. Tree of all existing active sets s for system shown in article Fig. (3). In set 1 all $x_i > 0$, yellow background stand for complex leading eigenvalues of the active interaction matrix. Black indicates that the agent associated with that index is not active. The gray lines indicate to all possible switching events where the number of active agents N_{act} changes ± 1. Blue arrows mark the observed sequence of the dynamics for the examples Eq. (8) with $D = -A_{ii} = 0.14$.

Materials and Methods

Eigenvalues

The eigenvalues $\Lambda \in \mathbb{C}$ and eigenvectors v of a matrix A are defined as solutions of the matrix equation $\Lambda v = Av$. The solution of a linear differential equation $\dot{x} = A(x - x^*)$ is of the form $x(t) - x^* = \exp(At)(x(0) - x^*)$. For large times the $x(t)$ will therefore point into the direction of the eigenvector v_1 with the eigenvalue Λ_1 with the largest real part and $(x(t) - x^*) \sim \exp(\Lambda_1 t)v_1$ as t gets large. If the largest real part of Λ_1 is larger (smaller) than zero $|x(t) - x^*|$ will grow (decay) exponentially and x^* is an unstable (stable) fixed point of the differential equation.

Fixed points and attractors

Let L^s_{act} be the maximal real part of the leading eigenvalue of the active interaction matrix A^s_{act} associated with the active subset s. The effective fixed point $x^{*\,s}_{\text{act}}$ is *stable* and perturbations of concentrations vanish if $L^s_{\text{act}} < 0$. The fixed point is *accessible* if x^s_{act} approaching $x^{*\,s}_{\text{act}}$ does not cause a switching event and *inaccessible* otherwise. Stationary solutions of a sequentially linear system therefore require fixed points that are both stable and accessible.

Periodicity of attractors and self-organized criticality

Suppose a bounded attractor exists for a sequentially linear system with N agents i. The perturbation $x(t) \to x'(t)$ at time $t = t_0$ also effects later switching times of agents i, i.e. $t_m \to t'_m$ such that $|\tau'_m - \tau_m| < C|\delta x_m|$ for some constant $C > 0$, where $\delta x_m = x'(t'_m) - x(t_m)$. Since $|\delta x_m| \to 0$ sufficiently fast as $m \to \infty$ (there exists an attractor) the cumulated time shift $t'_m - t_m$ of switching times remains finite for all times. This shows that the perturbed x' behaves (after some time) just like the unperturbed x only shifted in time. Perturbation neither vanishes nor grow exponentially, and the Lyapunov exponent can only be zero ($\lambda = 0$). Moreover, since the number of active sets is finite (2^N) and the dynamics is bounded the concentrations have to return to values on the attractor with arbitrary precision within

some finite return-time. The remaining concentration difference can be seen as a perturbation so that the attractor can only be a periodic cycle. The time-shift produces a phase-shift of the periodic dynamics.

Stability: the maximum Lyaponov exponent

While eigenvalues tell us something about the stability of a fixed point the Lyaponov exponent λ tells something about the stability of the dynamics $x(t)$ itself. The Lyapunov exponent $\lambda = \lim_{t\to\infty} \log(|\delta x(t)|)/\log(|\delta x(0)|)$ measures how a small perturbation $\delta x(t)$ grows with time. If $\lambda < 0$ the perturbation vanishes exponentially with time or grow exponentially if $\lambda > 0$. System with $\lambda > 0$ are chaotic (in-stable dynamics extremely sensitive to noise or perturbations) while $\lambda < 0$ indicates stable dynamics insensitive to perturbations and noise. Systems with $\lambda = 0$ are special as their dynamics is sensitive to noise and perturbations without "overreacting" like chaotic systems. These systems at the "edge of chaos" adapt to fluctuations but remain close to their unperturbed dynamics.

Temporal self-organization of switching events

Here we derive a simple approximation of the Lyapunov exponent of sequentially linear dynamics which explains temporal self-organization quantitatively. This is necessary for understanding why switching in general happens between active networks with stable and unstable dynamics and not from one stable stable (unstable) to another stable (unstable) active network.

Qualitative analysis of bounded attractors of sequentially linear dynamics has shown that the attractor is periodic and the Lyapunov exponent $\lambda = 0$. Characteristic information on the dynamics gets encoded by periodic sequences $(\tau_m,\, L^{s_m}_{\rm act})$, $m = 1, 2, \ldots$ with a period of some length q such that $\tau_{m+q} = \tau_m$ and $s_{m+q} = s_m$ (for large enough m) as in the example shown in Fig. (1) in the main article. If the dynamics of the system would remain in an active network $L^s_{\rm act}$ the Lyapunov exponent would be identical with the largest real part $L^s_{\rm act}$ of the eigenvalues of A. The Lyapunov exponent λ of the sequentially linear system therefore is well approximated[1] by the time average over $L^{s_m}_{\rm act}$, i.e.

$$\lambda \sim \lim_{m\to\infty} \frac{1}{Z_m} \sum_{n=1}^{m} \tau_n L^{s_n}_{\rm act} \qquad Z_m = \sum_{n=1}^{m} \tau_n \,. \tag{10}$$

Since the dynamics is periodic the time average only needs to be taken over one period and since $\lambda = 0$ one gets $0 \sim \sum_{k=1}^{q} \tau_{n+k} L^{s_{n+k}}_{\rm act}$ for n large enough. The "refocusing" mechanism discussed above qualitatively therefore is also "balancing" the times τ_m specific active sets s_m remain active by fine tuning switching times[2] such that contributions from time-domains with stable ($L^{s_m}_{\rm act} < 0$) and unstable dynamics ($L^{s_m}_{\rm act} > 0$) compensate each other. *Temporal balance* and *refocusing* are two aspects of the temporal self-organizing principle manipulating switching times.

Acknowledgments

This work has been funded by the *Forum Integrativmedizin* an initiative of the *Hilde Umdasch Privatstiftung*.

[1] Convergence of $x^s_{\rm act} \to x^{*\,s}_{\rm act}$ or into the direction of the leading possibly complex eigenvector, if $x^{*\,s}_{\rm act}$ is unstable, remains incomplete since convergence is always interrupted by a switching event.

[2] This also is supported by the fact that simulations with finite time increment regularly produce chaotic dynamics with small but positive Lyapunov exponents since switching times can only be tuned to the accuracy of the time increment. However λ approaches zero consistently as the time increment is made smaller and orbits become periodic again.

References

1. Hood L, Heath JR, Phelps ME, Lin B (2004) Systems biology and new technologies enable predictive and preventative medicine. *Science* 306:640–643.

2. Gavin AC, Aloy P, Grandi P, Krause R, Boesche M, et al. (2006) Proteome survey reveals modularity of the yeast cell machinery. *Nature* 440:631–636.

3. Kashtan N, Alon U (2005) Spontaneous evolution of modularity and network motifs. *Proc Natl Acad Sci USA* 102:13773–13778.

4. de Chassey B, Navratil V, Tafforeau L, Hiet MS, Aublin-Gex A, et al. (2008) Hepatitis C virus infection protein network. *Mol Syst Biol* 4:230.

5. Church GM (2005) From systems biology to synthetic biology. *Mol Syst Biol* 1:0032.

6. Greer EL, Brunet A (2005) FOXO transcription factors at the interface between longevity and tumor suppression. *Oncogene* 24:7410–7425.

7. Tothova Z, Gilliland DG (2007) FoxO Transcription Factors and Stem Cell Homeostasis: Insights from the Hematopoietic System. *Cell Stem Cell* 1:140–152.

8. Burg MB, Kwon ED, Kultz D (1996) Osmotic regulation of gene expression. *Faseb J* 10:1598–1606.

9. Capaldi AP, Kaplan T, Liu Y, Habib N, Regev A, et al. (2008) Structure and function of a transcriptional network activated by the MAPK Hog1. *Nature Genetics* 40:1300–1306.

10. Pirkkala L, Nykanen P, Sistonen L (2001) Roles of the heat shock transcription factors in regulation of the heat shock response and beyond. *The FASEB Journal* 15:1118–1131.

11. Beer MA, Tavazoie S (2004) Predicting gene expression from sequence. *Cell* 117:185–198.

12. Das D, Banerjee N, Zhang MQ (2004) Interacting models of cooperative gene regulation. *Proc Natl Acad Sci USA* 101:16234–16239.

13. Gertz j, Siggia ED, Cohen BA, (2009) Analysis of Combinatorial cis-Regulation in Synthetic and Genomic Promoters. *Nature* 457:215–218.

14. Vokes SA, Ji H, Wong WH, McMahon AP (2008) A genome-scale analysis of the cis-regulatory circuitry underlying Sonic hedgehog-mediated patterning of the mammalian limb. *Genes Dev.* 22:2651–2663.

15. Visel A, Blow MJ, Li Z, Zhang T, Akiyama JA, et al. (2009) ChIP-seq accurately predicts tissue-specific activity of enhancers. *Nature* 457:854–858.

16. Zinzen RP, Girardot C, Gagneur J, Braun M, Furlong EEM (2009) Combinatorial binding predicts spatio-temporal cis-regulatory activity. *Nature* 462:65–70.

17. Lee TI, Rinaldi NJ, Robert F, Odom DT , Bar-Joseph Z, et al. (2002) Transcriptional Regulatory Networks in Saccharomyces cerevisiae. *Science* 298:799–804.

18. Guet CC, Elowitz MB, Hsing W, Leibler S (2002) Combinatorial synthesis of genetic networks. *Science* 296:1466–1470.

19. Kitano H (2002) Computational systems biology. *Nature* 420:206–210.

20. Semsey S, Andersson AM, Krishna S, Jensen MH, Massé E, et al. (2006) Genetic regulation of fluxes: iron homeostasis of Escherichia coli. *Nucl Acids Res* 34:4960–4967.

21. Ozbudak EM, Thattai M, Lim HN, Shraiman BI, van Oudenaarden A (2004) Multistability in the lactose utilization network of Escherichia coli. *Letters to NATURE* 427:237–240.

22. Smolen P, Baxter DA, Byrne JH (1998) Frequency selectivity, multistability, and oscillations emerge from models of genetic regulatory systems. *Am J Physiol Cell Physiol* 274:C531–C542.

23. Park JH, Helfrich-Förster C, Lee G, Liu L, Rosbash M, et al. (2000) Differential regulation of circadian pacemaker output by separate clock genes in Drosophila. *Proc Natl Acad Sci USA* 97:3608–3613.

24. Hoffmann A, Levchenko A, Scott ML, Baltimore D (2002) The IκB-NκB Signaling Module:Temporal Control and Selective Gene Activation. *Science* 298:1241–1245.

25. Métivier R, Penot G, Hübner MR, Reid G, Brand H, et al. (2003) Estrogen Receptor- Directs Ordered, Cyclical, and Combinatorial Recruitment of Cofactors on a Natural Target Promoter. *Cell* 115:751–763.

26. Métivier R, Penot G, Carmouche RP, Hubner MR, Reid G, et al. (2004) Transcriptional complexes engaged by apo-estrogen receptor-alpha isoforms have divergent outcomes. *EMBO J* 23:3653–3666.

27. Luscombe NM, Babu MM, Yu H, Snyder M, Teichmann SA, et al. (2004) Genomic analysis of regulatory network dynamics reveals large topological changes. *Letters to NATURE* 413:308–312.

28. Amorim MJ, Cotobal C, Duncan C, Mata J (2010) Global coordination of transcriptional control and mRNA decay during cellular differentiation. *Mol Syst Biol* 6:380.

29. Lee JE, Lee JY, Wilusz J, Tian B, Wilusz CJ (2010) Systematic Analysis of Cis-Elements in Unstable mRNAs Demonstrates that CUGBP1 Is a Key Regulator of mRNA Decay in Muscle Cells. *PLOS ONE* 5:e11201.

30. Ciechanover A (2006) Intracellular protein degradation: from a vague idea thru the lysosome and the ubiquitin-proteasome system and onto human diseases and drug targeting. *Exp Biol Med* 231:1197–1211.

31. Gsponer J, Futschik ME, Teichmann SA, Babu MM (2008) Tight Regulation of Unstructured Proteins: From Transcript Synthesis to Protein Degradation. *Science* 322:1365–1368.

32. Bossi A, Lehner B (2009) Tissue specificity and the human protein interaction network. *Mol Syst Biol* 5:260.

33. Burkard TR, Planyavsky M, Kaupe I, Breitwieser FP, Bürckstümmer T, et al. (2011) Initial characterization of the human central proteome. *BMC Syst Biol* 5:17.

34. Turner TE, Schnell S, Burrage K (2004) Stochastic approaches for modelling in vivo reactions. *Computational Biology and Chemistry* 28:165–178.

35. Bratsun D, Volfson D, Tsimring LS, Hasty J (2005) Delay-induced stochastic oscillations in gene regulation. *Proc Natl Acad Sci USA* 102:14593–14598.

36. Paulsson J, Berg OG, Ehrenberg M (2000) Stochastic focusing: Fluctuation-enhanced sensitivity of intracellular regulation. *Proc Natl Acad Sci USA* 97:7148–7153.

37. Langton CG (1990) Computation at the edge of chaos. *Physica D* 42:12–37.

38. Mitchell M, Hraber PT, Crutchfield JP (1993) Revisiting the Edge of Chaos: Evolving Cellular Automata to Perform Computations. *Complex Systems* 7:89–130.

39. Kauffman SA (1993) *The Origins of Order- Self-Organization and Selection in Evolution.* (Oxford University Press).

40. Bhattacharjya A, Liang S (1996) Power-law distributions in some random Boolean networks. *Phys Rev Lett* 77:1644–1647.

41. Glass L, Hill C (1998) Ordered and disordered dynamics in random networks. *Europhys Lett* 41:599–604.

42. Shmulevich I, Lähdesmäki H, Dougherty ER, Astola J, Zhang W (2003) The role of certain Post classes in Boolean network models of genetic networks. *Proc Natl Acad Sci USA* 100:10734–10739.

43. Stokić D, Hanel R, Thurner S (2008) Inflation of the edge of chaos in a simple model of gene interaction networks. *Phys Rev E* 77:061917.

44. Hanel R, Pöchacker M, Thurner S (2010) Living on the edge of chaos: minimally nonlinear models of genetic regulatory dynamics. *Phil Trans Roy Acad Sci A* 368:5583–5596.

45. Glass L, Kauffman SA (1973) The logical analysis of continuous non-linear biochemical control networks. *J Theor Biol* 39:103–129.

46. Qian X, Ghaffari N, Ivanov I, Dougherty ER (2010) State reduction for network intervention in probabilistic Boolean networks. *Bioinformatics* 26:3098–3104.

47. de Jong H, Geiselmann J, Hernandez C, Page M (2003) Genetic network analyzer: qualitative simulation of genetic regulatory networks. *Bioinformatics* 19:336–344.

48. Viretta AU, Fussenegger M (2004) Modeling the quorum sensing regulatory network of human-pathogenic Pseudomonas aeruginosa. *Biotech Prog* 20:670–678.

49. Ropers D, de Jong H, Page M, Schneider D, Geiselmann J (2006) Qualitative simulation of the carbon starvation response in Escherichia coli. *Biosystems* 84:124–152.

50. Rewieński M, White J (2003) A trajectory piecewise-linear approach to model order reduction and fast simulation of nonlinear circuits and micromachined devices. *IEEE/ACM Transactions on Computer-Aided Design of Integrated Circuits and Systems* 252-257.

51. Yagil G, Yagil E (1971) On the relation between effector concentration and the rate of induced enzyme synthesis. *Biophys J* 11:11–27.

52. Ptashne M (1992) *A genetic switch: phage λ and higher organisms. Blackwell Science & Cell Press.*

53. Casey R, de Jong H, Gouzé JL (2006) Piecewise-linear Models of Genetic Regulatory Networks: Equilibria and their Stability. *J Math Biol* 52:27–56.

54. Pigolotti S, Krishna S, Jensen MH (2009) Symbolic Dynamics of Biological Feedback Networks. *Phys Rev Lett* 102:088701.